Methods 238 (2025) 27–39

Contents lists available at ScienceDirect

Methods

journal homepage: www.elsevier.com/locate/ymeth

Two minimally invasive strategies to implant guide cannulas for multiple injections in deep brain areas☆

Stefania Bartoletti [a], Federica Raimondi [a], Beatrice Casadei Garofani [a], Elisa Ren [a], Francesca Ciarpella [b], Arianna Capodiferro [a], Gemma Palazzolo [c], Antonietta Vilella [a], Giuseppina Leo [a], Michele Zoli [a], Ilaria Decimo [b], Giulia Curia [a,*]

[a] Department of Biomedical, Metabolic and Neural Sciences, University of Modena and Reggio Emilia (UNIMORE), Modena, Italy
[b] Department of Diagnostics and Public Health, University of Verona (UNIVR), Verona, Italy
[c] Italian Institute of Technology (IIT), Genova, Italy

ARTICLE INFO

Keywords:
3Rs principle
Guide cannula implantation
Minimally invasive surgeries
Multiple intracranial injections
Pilocarpine model
Preclinical *in vivo* studies
Refinement
Stereotaxic surgery

ABSTRACT

Temporal lobe epilepsy (TLE) is characterized by seizures that originate in temporal structures and that are pharmacoresistant in ~ 40 % of patients. In the context of a preclinical study aimed at developing an innovative therapy to treat TLE, we needed to perform multiple intracranial injections in the rat ventral CA3 (vCA3). To reduce invasiveness and to increase the precision reproducibility when multiple injections are performed over time, we opted for the implantation of guide cannulas.

In the conventional approach, the guide cannula is implanted close to the target zone damaging the brain tissue along the route of the cannula insertion. This is a particularly relevant issue in our study because vCA3 is situated deep in the rat brain. The damage caused by the standard procedure would severely compromise the integrity of the hippocampal tissue necessary for the effectiveness of the therapeutic intervention.

To overcome this problem, we developed, in TLE adult rats, two novel approaches to implant guide cannulas more superficially: the "above dentate gyrus (DG)" and the "above hippocampus (HPC)" strategies. The target brain area was then reached with the thinner infusion needle, resulting in minimally invasive approaches. We demonstrated by immunofluorescence that both novel surgical approaches enable injections of different agents into the ventral hippocampus with excellent precision and reproducibility. Being this aspect comparable between the two approaches, we concluded that the "above HPC" strategy must be preferred due to its lower invasiveness. Behavioral tests confirmed that memory, locomotion and anxiety level were not affected by the cannula-induced damage.

1. Introduction

Temporal lobe epilepsy (TLE) is a neurological disease characterized by the occurrence of spontaneous recurrent seizures that originate in the hippocampal and parahippocampal structures and temporal cortex. Up to 40 % of TLE patients are resistant to antiseizure medications and keep experiencing uncontrolled debilitating seizures. For these patients, resection of the epileptic focus, neurostimulation, or cell therapy represent the second-line therapeutic options [1,2]. In the context of a preclinical study aimed at investigating an innovative therapy intervention for the treatment of TLE [3], we encountered the need to perform multiple intracranial injections in the rat brain.

Abbreviations: AP, Anteroposterior; BSA, Bovine serum albumin; CMV, Cytomegalovirus; DAPI, 4,6-Diamidino-2-phenylindole, dihydrochloride; DG, Dentate gyrus; DV, Dorsoventral; FBR, Foreign body response; G, Gauge; GFAP, Glial fibrillary acidic protein; GFP, Green fluorescent protein; H&E, Hematoxylin & Eosin; HBSS, Hank's balanced salt solution; HPC, Hippocampus; IBO, Ibotenic acid; i.p., Intraperitoneal; M1, Primary motor cortex; ML, Mediolateral; MOI, Multiplicity of infection; NSCs, Neural stem cells; PFA, Paraformaldehyde; RT, Room temperature; SE, Status epilepticus; SEM, Standard error of the mean; s.c., Subcutaneous; TLE, Temporal lobe epilepsy; vCA3, ventral Cornu Ammonis 3.

☆ This article is part of a special issue entitled: 'Editors Collection - YMETH' published in Methods.

* Corresponding author at: University of Modena and Reggio Emilia, Department of Biomedical, Metabolic and Neural Sciences, Via G. Campi, 287, 41125 Modena, Italy.
E-mail address: gcuria@unimore.it (G. Curia).

https://doi.org/10.1016/j.ymeth.2025.03.005
Received 11 October 2024; Received in revised form 3 March 2025; Accepted 4 March 2025
Available online 8 March 2025

A cannula-based approach for direct injection into the brain is a precise and effective method used in preclinical studies to treat *in vivo* targeted brain regions while leaving the overall brain function unaffected [4]. This method can be useful to perform multiple infusions within the same brain area with a higher level of precision and with faster procedures, reducing therefore animal discomfort and post-surgical recovery time.

In the widely adopted approach for guide cannula implantation, the tip of the cannula is placed approximately 1 mm above the injection site [5–8], a strategy that comes with advantages and disadvantages. Compared to a previously tested strategy in which no space was left between the cannula tip and the injection site [9], the "1 mm approach" was correlated to minimal backflow contributing to a better distribution of infused agents [10]. This practice ensures a precise injection directly into the brain target zone although damaging the brain tissue encountered along the insertion route. We expected that the insertion of cannulas in deep areas of the brain, such as the ventral hippocampus, would massively damage the tissue possibly causing learning and memory deficits and psychiatric issues, all tasks related to the good functionality of the hippocampus and the limbic system. In addition, it has been shown that *in vivo* chronic implantation of a steel cannula in the rat primary motor cortex (M1) induced a complex foreign body response (FBR), characterized by glial scar tissue formation around the cannula associated with neuronal cell loss and leading to a deterioration in the execution of fine motor tasks [11]. The implantation of the guide cannula distant from the target area should avoid the formation of a glial scar in the target area and the impairment of its functionality.

In the present study, we present two novel approaches, the "above dentate gyrus (DG)" and the "above hippocampus (HPC)" strategies, to implant cannulas more superficially and to perform multiple injections into the vCA3 of epileptic rats. We investigated the level of precision reached by each strategy after multiple intracranial injections. We identified the strategy that provided the highest precision with the smallest damage and verified that it did not cause impairments in behavioral performances.

2. Materials and methods

2.1. Ethics statement

All animal experiments comply with ARRIVE (Animal Research: Reporting of In Vivo Experiments) guidelines [12–14]. All procedures were carried out in accordance with the European Directive 2010/63/EU [15]. The protocols approved by the Animal Welfare Body of the University of Modena and Reggio Emilia (UNIMORE) and of the University of Verona (UNIVR) were then authorized, respectively, by the Italian Ministry of Health (54/2019-PR) and by the Italian National Institute of Health (C46F4.N.N4E) according to the national guidelines on animal experimental research (art.31 legislative decree 26/2014). All efforts were made to refine procedures to improve animal welfare and reduce stress. Animal welfare was assessed and scored based on the Welfare Assessment Criteria that takes into account the FELASA (Federation of European Laboratory Animal Science Associations) recommendations [16,17]. Post-surgical pain was monitored for up to 3 days post-surgery, or longer if not resolved, and was scored using the rat Grimace scale [18,19]. Rats were implanted bilaterally to reduce the overall number of animals used.

2.2. TLE animal model

Sprague Dawley male rats (4 weeks old; Charles River Laboratories, Italy) arrived in the animal facility at UNIMORE and were housed in cages with environmental enrichment for their welfare, under controlled conditions (temperature 22 ± 1 °C, humidity 60 %), on a 12 h light/dark cycle, with food and water *ad libitum*. After a few days of habituation, rats were handled to familiarize themselves with the experimenter and reduce stress [20].

The day of the experiment, rats (140–160 g) were injected with scopolamine methyl nitrate (1 mg/kg, intraperitoneal – i.p.; S-2250, Merck, Germany) 30 min before pilocarpine (380 mg/kg, i.p.; P-6503, Merck, Germany) to prevent peripheral cholinergic side effects (e.g., excessive salivation, diarrhea etc.). Behavioral changes due to pilocarpine administration were monitored and scored using the Racine scale [21]. After a few min from pilocarpine injection, rats started experiencing acute epileptic seizures, initially not convulsive, then gradually becoming more severe (tonic-clonic seizures) and culminating in the *status epilepticus* (SE). To stop convulsive SE and reduce mortality, rats were injected with ketamine/diazepam (20/4 mg/kg i.p.) 30 min after SE onset. The mortality rate acutely (within the first 72 h) after pilocarpine injection was 28 %. Rats not experiencing SE (13 %) were used in preliminary surgeries for procedure optimization (such as stereotaxic coordinate validation). A total of 54 epileptic rats underwent stereotaxic surgeries for bilateral cannula implantation and received intracranial injections of the agents; 51 were used for analysis (details are provided in Table 1 and Table 2), while 3 pilocarpine-treated rats were excluded from the analysis because of a premature headset loss (1 rat) and humane endpoint due to SE, a complication that is intrinsic to the pilocarpine model (2 rats). The experimental timeline is shown in Fig. 1.

2.3. Cannula preparation

Cannulas have been handcrafted by cutting a stainless-steel needle [9,22]. The cannula dimension was determined based on the minimal needle size for the efficient infusions of saline-based media, the viscous algal polysaccharide alginate used as biomimetic extracellular matrix, and neural stem cells (NSCs) without getting stuck in the needle; we opted for the combination guide cannula/infusion needle 22/27 gauge (G). The length of the guide cannulas was 9 mm for the "above DG" strategy and 7 mm for the "above HPC" strategy. To reach vCA3 at the correct depth in the brain, we used infusion needles 11 mm in length for both strategies.

2.4. Stereotaxic surgery for cannula implantation

Surgeries for the cannula implantation were performed bilaterally two weeks after SE (Fig. 1**a**). Before surgery, all tools were sterilized with ethanol 70 % for 30 min to reduce possible infections. The rat was weighed, anesthetized with isoflurane (4 % induction, 2 % mask, flow rate of 1.5 l/min) administered through an anesthesia machine equipped with isoflurane evaporator and flowmeter (MSS, UK), and with the oxygen producer (Drive DeVilbiss Healthcare Ltd., UK) and Fluovac System (Harvard Bioscience, USA). Rats were injected with an anti-inflammatory drug (Carprofen 5 mg/kg, subcutaneous – s.c.) and subsequently fixed in position with the head on a stereotaxic apparatus (David Kopf Instruments, USA). The head was shaved, and the scalp was disinfected with an antiseptic solution of povidone-iodine 10 % (Betadine) and injected with a local anesthetic (Lidocaine 2 %, 200 μl, s.c.). We waited until the rat's breathing was stable before proceeding; this required several minutes due to the challenges posed by the epileptic condition. The skull was then exposed through a midline incision, scratched, cleaned to remove the periosteum, and rubbed with silver powder to reduce bleeding and risk of infections. A micro-drill and stainless-steel burrs (tip 0.9 mm diameter, Fine Science Tools GmbH, Germany) were used to perform two bilateral craniotomies according to the rat atlas [23] in stereotaxic coordinates: anteroposterior (AP) −5.5 mm from Bregma, mediolateral (ML) ± 4.5 mm from midline for rats weighing ≤ 285 g or ± 4.8 mm for rats weighing > 285 g. Two more craniotomies were made for anchor screws (1 mm diameter, Bilaney Consultants GmbH, Germany) to improve the stability of the implant. The 22 G cannulas were placed in position over the craniotomies and gently lowered into the brain after cutting the dura mater according to the following dorsoventral (DV) coordinates: −3.5 mm from the dura

Table 1
Experimental groups used for precision score and cannula-induced damage analyses.

	Rat ID	Treatment	First Inj.	Second Inj.	Third Inj.	Above DG Precision Score (left hemisphere)	Above HPC Precision Score (right hemisphere)
BATCH 1	1	Pilo	IBO	NSCs		0	0
	2	Pilo	IBO	NSCs		4	4
	3	Pilo	IBO	NSCs		4	4
	4	Pilo	IBO	NSCs + Alg	Alg	3	4
	5	Pilo	IBO	NSCs + Alg	Alg	1	3
	6	Pilo	IBO	NSCs + Alg	Alg	1	3
	7	Pilo	IBO	NSCs + Alg	Alg	1	4
	8	Pilo	IBO	Alg	Alg	2	4
	9	Pilo	IBO	Alg	Alg	1	3
	10	Pilo	IBO			4	0
	11	Pilo	IBO			3	2
	12	Pilo	IBO	NSCs + Alg	Alg	1	3
	13	Pilo	IBO	NSCs + Alg	Alg	0	4
	14	Pilo	IBO	NSCs + Alg	Alg	0	4
	15	Pilo	IBO	NSCs + Alg	Alg	3	2
	16	Pilo	IBO	NSCs + Alg	Alg	0	0
	17	Pilo	IBO	NSCs		4	2
	18	Pilo	IBO	NSCs		3	0
	19	Pilo	IBO	Alg		0	4
	20	Pilo	IBO	Alg		4	3
	21	Pilo	IBO	Alg		1	3
BATCH 2	22	Pilo	IBO	NSCs + Alg		2	2
	23	Pilo	IBO	NSCs + Alg		2	2
	24	Pilo	IBO	Alg		4	4
	25	Pilo	IBO	Alg		4	0
	26	Pilo	IBO	NSCs		4	4
	27	Pilo	IBO	NSCs		4	4
	28	Pilo	IBO	NSCs + Alg		3	4
	29	Pilo	IBO	NSCs + Alg		3	4
	30	Pilo	IBO	NSCs + Alg		0	4
	31	Pilo	IBO	NSCs		3	4
	32	Pilo	IBO	NSCs + Alg		3	4
	33	Pilo	IBO	NaCl/HEPES		4	4
	34	Pilo	IBO	NaCl/HEPES		1	2
	35	Pilo	IBO	Alg		3	3
	36	Pilo	IBO	Alg		4	0
	37	Pilo	IBO	NSCs		0	0
	38	Pilo	IBO	NSCs		3	3
	39	Pilo	IBO	NSCs		3	3
	40	Pilo	IBO	NSCs + Alg		0	4
	41	Pilo	IBO	NaCl/HEPES		4	0

Experimental groups used for precision score (Fig. 3) and cannula-induced damage (Fig. 4) analyses. Treatment, infusions received, and precision scores are provided for each rat implanted with the two surgical strategies for cannula implantation. Alg: Alginate; DG: Dentate gyrus; HPC: Hippocampus; IBO: Ibotenic acid; Inj: Injection; NSC: Neural stem cells; Pilo: Pilocarpine.

mater in one hemisphere for the "above DG" strategy, and −1.5 mm in the contralateral hemisphere for the "above HPC" strategy (Fig. 2**, top row**). Cannulas and anchors were fixed in position with ethyl-cyanoacrylate and dental cement (Fig. 1**a**). To avoid cannula clogging, a stainless-steel obturator (stylet) was made starting from a Hamilton's needle cleaning kit (part 18304, Hamilton Company, USA) and inserted into each guide cannula. At the end of the surgical procedure, which lasted approximately 75 min, isoflurane was lowered to 0 % and we let the rat breathing oxygen 100 % before completely disconnecting it from the anesthesia machine; meanwhile, anti-inflammatory (Carprofen 5 mg/kg, s.c.) and antibiotic (Enrofloxacin 5 mg/kg, s.c.) drugs were administered to reduce post-surgical pain and risk of infection, and sterile saline (NaCl 0.9 %, 0.5 ml, s.c.) was injected to rehydrate the rat. An anesthetic and antimicrobial gel (Lidocaine 2.50 g, Neomycin 0.50 g, Fluocinolone 0.025 g) was applied between the cement and the skin around the wound. The animal was moved into its home cage and monitored until full recovery from anesthesia; respiratory functionality and behavior were monitored and recorded on the rat clinical report upon awakening or/and until normalization (usually within 5 min). Pain level was scored over the three days post-surgery, or longer if not resolved, using the rat Grimace scale [18].

2.5. Solutions intracerebrally injected

The solutions and the biological materials to be injected in the vCA3 were prepared in sterile conditions as described below. Products were purchased from Merck Life Science (Italy), unless specified.

2.5.1. Ibotenic acid

The cytotoxic agent ibotenic acid (IBO; code Tocris Bioscience 0285/5, Bio-Techne SRL, USA) was resuspended with sterile PBS and sonicated for 3 min to reach the final concentration of 1 mg/ml (pH 7.4). The stock solution was aliquoted and stored at −20 °C. On the day of the injection, one aliquot was thawed and used without refreezing.

2.5.2. Alginate

The algal polysaccharide alginate (DuPont Nutrition Norge – NovaMatrix, Norway) was labelled with the red-fluorescent tag Alexa Fluor 568 (ThermoFisher Scientific, USA) using the EDC-NHS chemistry [25,26] to monitor its localization after injection in the rat brain. Marked alginate was freeze dried, irradiated with UV ($\lambda = 360$ nm) for 30 min, then it was resuspended in NaCl/HEPES/$CaCl_2$ 135/20/2 mM (pH 7.4) to obtain a 0.8 % (weight/volume) stock solution, and sterile filtered (0.2 μm).

Table 2
Experimental groups used for behavioral tests.

	Rat ID	Treatment	Strategy for Bilateral Cannula Implantation	Injection
Implanted and injected epileptic rats	42	Pilo	Above HPC	IBO
	43	Pilo	Above HPC	IBO
	44	Pilo	Above HPC	IBO
	45	Pilo	Above HPC	IBO
	46	Pilo	Above HPC	IBO
	47	Pilo	Above HPC	IBO
	48	Pilo	Above HPC	IBO
	49	Pilo	Above HPC	IBO
	50	Pilo	Above HPC	IBO
	51	Pilo	Above HPC	IBO
Control group (naïve rats)	52			
	53			
	54			
	55			
	56			
	57			
	58			
	58			

Experimental groups used for behavioral tests analysis (Fig. 5). Treatment and infusions received are provided for each rat bilaterally implanted with cannulas using the "Above HPC" strategy. Control group includes naïve non-epileptic, not implanted and not injected rats. HPC: Hippocampus; IBO: Ibotenic acid; Pilo: Pilocarpine.

2.5.3. Rat hippocampal NSCs

At UNIVR, pregnant female Sprague Dawley rats were anesthetized (isoflurane 4 %) and sacrificed by cervical dislocation on the 18th day of gestation. The embryos were extracted and placed on a Petri dish kept on ice and dissected to obtain their brain, isolate the hippocampus and transfer them in a centrifuge tube with Hank's Balanced Salt Solution (HBSS). The extracted tissue was washed in HBSS (3 times), treated with trypsin at 37 °C for 10 min, washed again in HBSS (3 times), and then mechanically dissociated using Pasteur pipettes. The NSCs were cultured in suspension in T75 flasks (Falcon) to obtain neurospheres that, 7–10 days later, were collected, centrifuged, and mechanically dissociated to a single-cell suspension [27]. Single NSCs were infected at a multiplicity of infection (MOI; infectious units per cell) of 2 with a lentivirus carrying the green fluorescent protein (GFP) reporter gene under cytomegalovirus (CMV) promoter (LV00926Z, Creative Biogene, USA). NSCs were then grown in suspension and one week before *in vivo* injections were transferred from UNIVR to UNIMORE using a portable incubator (model CellTrans 2018, Labotect, Germany).

2.6. Intrahippocampal injections through the guide cannula

Intrahippocampal injections were started one week after the cannula implants. The infusion needle (27 G), whose length was adjusted to reach the vCA3 (DV −5.5 mm) [23] and verified by a calliper, was glued with a 0.46 x 0.91 mm polyethylene tube (Phymep, France). Milli-Q water was used to test the good quality of the seal verifying no leaking occurred between the two parts. The infusion system (needle + tube; Fig. 1**b**) was then attached with hot glue to a Hamilton syringe (10 µl Gastight 1801 RN, Hamilton Company, Switzerland); both were filled with Milli-Q water and placed into a syringe pump (Legato, KD Scientific Inc., USA). The syringe plunger was pushed to empty the Hamilton and check the connection quality (no leaking), and then pulled to fill the syringe with 0.1 µl of air followed by the solution to be infused.

The rat was weighed, anesthetized with isoflurane through an anesthesia machine (4 % induction, 2 % mask, flow rate of 1.5 l/min) and injected with an anti-inflammatory drug (Carprofen 5 mg/kg, s.c.). The stylet was removed from each guide cannula, and the infusion needle was slowly inserted manually. The solution was infused at a speed of 1 µl/min. Infusion needles were left in place 5 min after the injection was completed to avoid backflow and then they were slowly removed. To prevent clogging until the next injection, an obturator was inserted into each guide cannula. At the last infusion, a cap made of hot glue was placed to close the guide cannula preventing dust entrance and reducing the risk of infections. At the end of the infusion, isoflurane was lowered to 0 % and we let the rat breathing oxygen 100 % before completely disconnecting it from the anesthesia machine; meanwhile, antibiotic (Enrofloxacin 5 mg/kg, s.c.) and anti-inflammatory (Carprofen 5 mg/kg, s.c.) drugs were administered to reduce postsurgical pain and the risk of infection, and sterile saline (NaCl 0.9 %, 0.5 ml, s.c.) was injected to rehydrate the rat. An anesthetic and antimicrobial gel (Lidocaine 2.50 g, Neomycin 0.50 g, Fluocinolone 0.025 g) was applied topically on the skin/tissue flaps around the implant. Rat was monitored until full recovery with particular attention to respiratory rate and behavior upon awakening from anesthesia. Rats were monitored daily, and pain level was scored using the rat Grimace scale [18] for the 3 days following the surgery, or longer if needed.

All rats were injected with IBO (1 mg/ml, 0.3–0.5 µl) to make room for subsequent infusion of NSCs avoiding an increase in the intracranial pressure and the contamination of the injected NSCs with the epileptic phenotype of the host brain cells. Four days after the IBO injection, when the acute inflammation was resolved and the chronic inflammation was not established yet [28], rats were randomly split into 4 experimental groups, and received one of the following injections: (i) alginate (2 or 8 µl), (ii) NaCl/HEPES (8 µl), (iii) NSCs ($0.75\text{-}1{\cdot}10^6$ NSCs in NaCl/HEPES, final volume 5–8 µl), (iv) NSCs + alginate ($0.75\text{-}1{\cdot}10^6$ NSCs in alginate, final volume 5–8 µl).

2.7. Perfusion and tissue collection

At 4, 8 or 13 weeks after the last intracerebral infusion, rats were sacrificed by anesthesia with inhaled isoflurane and transcardially perfused with a saline solution containing NaCl 0.9 % and $CaCl_2$ 2 mM to wash out the blood. Rats were then perfused with paraformaldehyde (PFA) 4 % in NaCl/HEPES/$CaCl_2$ 135/20/2 mM, pH 7.4, and sucrose 4 % to fix the tissues. Brains were collected and post-fixed in PFA 4 % at 4 °C for 24 h, followed by cryoprotection in a sterile solution of sucrose 30 % in NaCl/HEPES/$CaCl_2$ at 4 °C. The samples were then frozen at −80 °C, coronally sliced (thickness 30–35 µm) with a cryostat (model CM1520, Leica, Germany), and brain slices were stored at −20 °C in an anti-freeze cryoprotectant solution (NaCl/HEPES/$CaCl_2$ + glycerol, 1:1).

2.8. Histology

2.8.1. Hematoxylin & Eosin (H&E) staining

To perform the H&E staining, brain slices lying on glass slides were submerged in NaCl/HEPES/$CaCl_2$, 135/20/2 mM then in Mayer's Hematoxylin 0.1 % (O.Kindler, Orsatec, Germany, ready to use), and then rinsed in Milli-Q water before being soaked in Eosin-solution 0.2 % (O. Kindler, Orsatec, Germany, ready to use). The slides were then rinsed in Milli-Q and dipped in ethanol at increasing concentrations, 50 %, 70 %, 90 % and 100 %. Finally, they were dipped in Xylene, mounted with Eukitt (15320, Electron Microscopy Sciences, USA) covered with glass, and left to dry overnight.

2.8.2. Immunofluorescence staining

Immunofluorescence staining was performed in free-floating brain slices using a multi-well tray on an orbital shaker (120 rpm, Incofar, Italy). Brain slices were washed with NaCl/HEPES/$CaCl_2$ 135/20/2 mM (3x10 min) solution at room temperature (RT). Pre-incubation blocking was made with NaCl/HEPES/$CaCl_2$ 135/20/2 mM solution, Triton X-100 0.5 % and BSA 2 % (Merck, Germany) for 1 h, at RT. Sections were then incubated with primary antibodies in a blocking solution overnight at 4 °C. The day after, sections were washed in blocking solution w/o bovine serum albumin (BSA) (3x10 min, RT) before incubating with

Fig. 1. Experimental procedures. On the top, the timeline of the experimental procedures is shown based on rats' ages. In the *inset a*, pictures show the surgical implantation into the rat brain of the guide cannulas (left) that are subsequently cemented in place (right). In the *inset b*, pictures show the infusion set up and the system made of needles + tubing connected to a syringe pump.

secondary antibody in blocking solution w/o BSA for 3 h, at RT, in a dark room to avoid signal bleaching. Slices were then washed in blocking solution w/o BSA (3x10 min, RT) and with NaCl/HEPES/$CaCl_2$ 135/20/2 mM solution (1x10 min, RT), mounted on glasses, coverslipped and sealed with DAPI Fluoromount-G (Southern Biotech, USA). Slides were stored in dark boxes at 4 °C.

2.8.3. Antibodies

The following primary antibodies were used: anti-GFP (AMab13970 Abcam Limited, UK, chicken, 1:200), anti-NeuN (MAB377 Merck, Germany, mouse, 1:200), and anti-GFAP (Z0334 Dako, Agilent, USA, rabbit, 1:2000). The secondary antibodies used were donkey anti-rabbit Alexa Fluor 488 (A21206 Thermo Fisher Scientific, USA, donkey, 1:400), goat anti-chicken Alexa Fluor 488 (A11039 Thermo Fisher Scientific, USA, goat, 1:400) and donkey anti-mouse Alexa Fluor 546 (A10036 Thermo Fisher Scientific, USA, donkey, 1:400). DAPI (Southern Biotech, USA) was used for cell nuclei staining.

2.9. Images capture and measurements

Images of brain slices were acquired with the Eclipse Ci-L upright microscope (Nikon Corporation, Japan), equipped for both brightfield and fluorescence images. Images were analyzed at 4x magnification and captured at 10x or 20x magnification using NIS Elements Basic Research Software (Nikon Corporation, Japan).

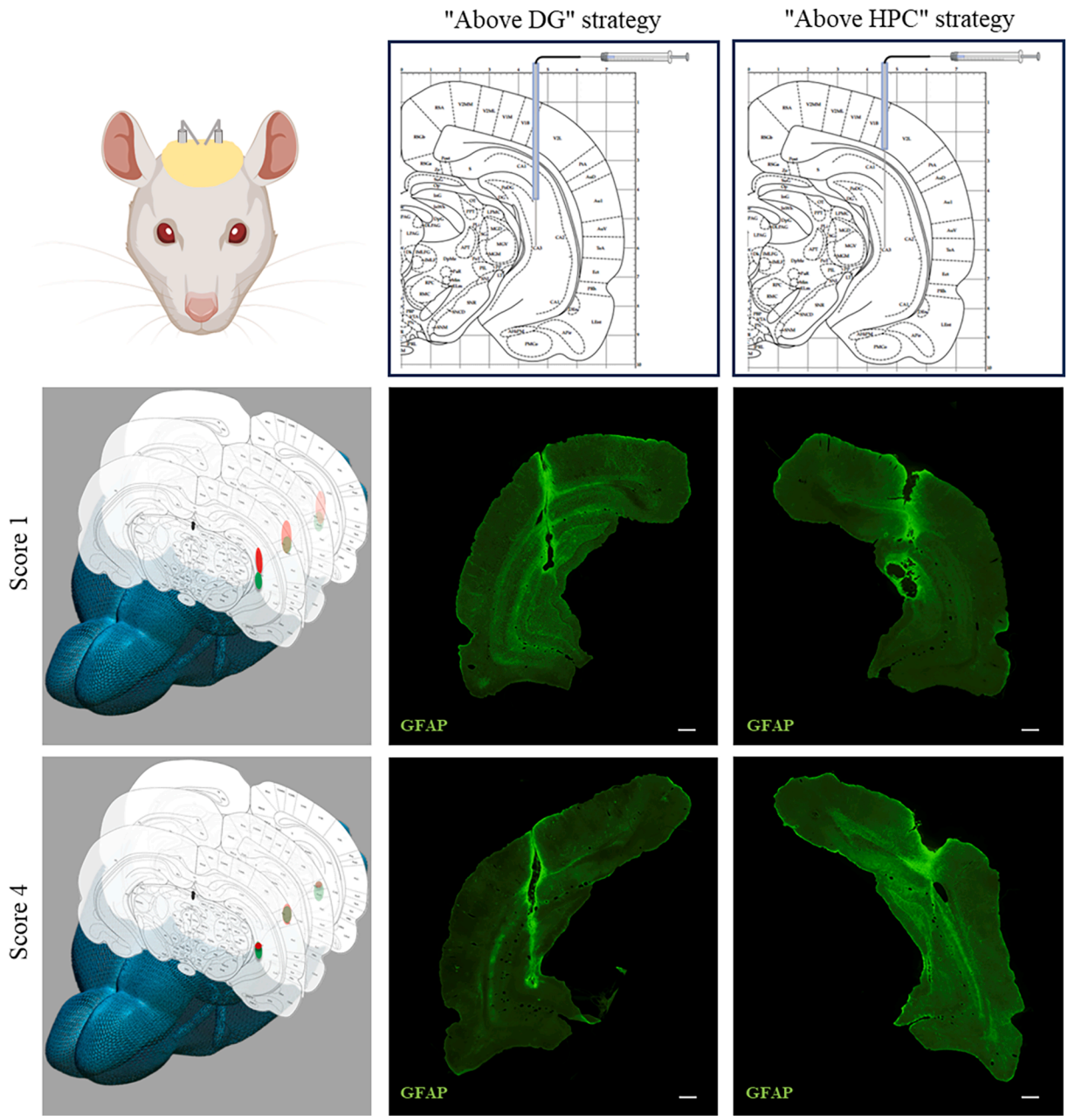

Fig. 2. Novel surgical strategies and precision score methodology. Image on the left upper row shows a schematic of a rat bilaterally implanted with guide cannulas (created with BioRender). On the right, coronal brain schemes illustrating the surgical strategies for guide cannula implantation with the "above DG" strategy and the "above HPC" strategy (modified from Rat Brain Atlas online free version [24] with BioRender). Middle and lower rows show the analysis method to score the precision accuracy. On the left panels graphical representations of scores 1 and 4, respectively, are reported. The green dots represent the target vCA3 area at each specific AP value, while the lesion/fluorescent area is marked in red. It is possible to appreciate that in the "score 4" example the injection site perfectly matched the target area, while in the "score 1" example the lesion/fluorescence only marginally reached vCA3 (created with PowerPoint combining images from Rat Brain Atlas [24] and KellyBullockArt [29] online free versions). Middle and right panels are representative immunofluorescence images of coronal brain sections (10x objective, scale bars 500 μm) showing the position accuracy scores 1 and 4 of both cannula implant strategies. GFAP marks astrocytes in green. DG: dentate gyrus; GFAP: glial fibrillary acidic protein; HPC: hippocampus.

2.9.1. *Analysis of position accuracy*

The precision of the injection site was assessed by localizing the center of the lesion/fluorescent area (red spot in Fig. 2, grey panel) with respect to the target area vCA3 (green spot in Fig. 2, grey panel). We assigned a "position accuracy score" ranging from 0 (the injection site was wrong and far from the target area) to a maximum of 4 (the injection was perfectly centered in vCA3). The intermediate values were assigned when lesion/fluorescent areas only partially matched vCA3 (Fig. 2).

2.9.2. *Analysis of cannula-induced damage*

To evaluate cannula-induced damage, for each strategy, we quantified the percentage of rats with a damaged hippocampus and the percentage of those presenting an intact hippocampus; in this latter case, the damage was limited to the cortex.

2.10. *Behavioral tests*

Behavioral studies were conducted in a separate batch of TLE rats (n = 10), bilaterally implanted with the "above HPC" strategy, and injected

in vCA3 with IBO (1 mg/ml, 3 μl) (Table 2). Naïve animals served as controls (n = 8). The series of behavioral tests conducted 4 weeks after cannula implantation are associated with memory and spatial learning (novel object location test), motor ability (open field test), and anxiety behavior (open field and light/dark box test). Between consecutive tests, a 3–4-day washout period was allowed.

Animals were handled weekly before starting the behavioral tests to reduce the animal stress level. Animals were placed in the test room at least 30 min to 1 h before beginning the procedures. All behavioral apparatuses were thoroughly cleaned between each rat performance using ethanol 70 % to minimize bias due to olfactory cues [30]. Animals that experienced epileptic seizures during the behavioral tests were excluded from the statistical analyses. All performances were recorded by video-tracking and quantified using ANY-maze Software version 7.16 (Stoelting Company, USA).

2.10.1. Novel object location test

The arena was 100 × 70 cm (wall height 38 cm). One rat at a time was habituated to the empty arena on days 1 and 2 freely to move for 10 min. On days 3 and 4 (training phase), the animal was placed in the arena with two identical objects for 10 min. The objects consisted of 2 Lego blocks attached to the arena floor and placed 20 cm from the back and side arena walls. From the training phase on day 4, the memory test was performed three times after a variable retention interval of 2 h (short memory), 6 h (intermediate memory) and 24 h (long-term memory) [31]. In each memory test, one of the two objects was moved to a new position as schematic in Supplementary **Fig. S1A**. After each training/test session, the animal was returned to its home cage. The animal's performance was assessed by the time spent on the object located in the new location.

2.10.2. Open field test

Open field test corresponded to the 10 min free exploration of days 1 and 2 of the novel object location test. One animal at a time was placed in the center of the empty arena freely to move for 10 min (Supplementary **Fig. S1B left**). For evaluation, data were collected in the entire arena, further virtually divided into center, middle, periphery and corner areas (Supplementary **Fig. S1B right**). The travelled distance was assessed for the 2 days and was considered an indicator of locomotor activity. Time spent in the different arena subsegments was measured on day 1 and was used to estimate the anxiety level; increased anxiety results indeed in a preference for the borders of the arena.

2.10.3. Light/dark box test

The arena (78 × 98 cm with a wall height of 36 cm) was divided into a light zone and a dark zone (78 × 32 × 36 cm) obtained using black plastic inserts (Supplementary **Fig. S1C**). A small opening (10 × 10 cm) connected the light and dark areas. One rat at a time was placed in the light compartment of the arena and allowed to freely explore both rooms for 10 min. Anxious animals tended to spend more time in the dark area. We considered the latency of the first entry in the dark zone, the number of entries, and the time spent in the dark area.

2.11. Statistical analysis

Origin Pro 2024 (OriginLab, USA) software was used routinely during data analysis and graph plotting. Data were plotted as median and confidence interval [5–95] or mean ± standard error of the mean (SEM) and were considered statistically significant when $p < 0.05$.

3. Results

3.1. Precision of injections using the two novel surgical strategies for cannula implantation

In the context of a preclinical study aimed at investigating an innovative therapy to treat TLE [3], we needed to perform multiple intracranial injections. In these cases, injections through a guide cannula are recommended to guarantee high precision and reproducibility over time. The standard approaches for guide cannula implantation, consisting of positioning the cannula close to the target area (0–1 mm away), damage the brain tissue encountered along the insertion route, and, in case of injections in areas located deep in the brain, it can be massive [9] and compromise the functionality of a big portion of the brain. To overcome this problem, we developed two novel surgical strategies for cannula implantation with minimal invasiveness. The first approach, hereafter named "above DG" strategy, foresees the insertion of the guide cannula slightly deeper than the cortex while leaving the DG intact (Fig. 2**, top row**). The second approach, hereafter named "above HPC" strategy, foresees the implantation of the guide cannula even more superficially, within the cortex, leaving the whole hippocampal tissue intact (Fig. 2**, top row**).

Pilocarpine-treated rats were bilaterally implanted with guide cannulas inserted respectively with the "above DG" strategy in one hemisphere and with the "above HPC" strategy in the contralateral one. In our attempt to treat TLE, we needed to perform multiple injections in implanted rats: (i) IBO was used to create a niche where to accommodate NSCs avoiding intracranial pressure increase and contamination of the injected cells with epileptic endogenous cells; (ii) NSCs were injected with or without alginate, a biocompatible and low-immunogenic biopolymer shown to help survival and plasticity of transplanted cells [25]. The precise localization of the different agents was evaluated by assigning a position accuracy score in relation to the target area vCA3 (see Methods and Fig. 2) by immunofluorescence (Fig. 3**A-D**).

Our position accuracy analysis showed that vCA3 was correctly reached in 80.49 % of injections using both the "above DG" strategy and the "above HPC" strategy. The precision score was not statistically different between the two groups ("above DG": 3 [0–4], n = 41; "above HPC": 3 [0–4], n = 41; $p > 0.05$ Mann-Whitney; Fig. 3**E**).

3.2. Cannula-induced damage

H&E staining showed the mechanical damage induced by the cannulas (Fig. 4**A, B**). The brain slices obtained from rats receiving the cannula implantation with the "above DG" strategy show, as expected, damage in the cortex and in the more dorsal part of the hippocampus in 100 % of injections (Fig. 4**C**). The brain slices obtained from rats that were implanted with the "above HPC" strategy showed damage limited to the cortex, while the whole hippocampal structure was undamaged in 100 % of injections (Fig. 4**C**). These data indicated that the novel strategies developed in this study offer an improvement over the traditional standard approaches [9]. In particular, considering the similarities in the precision scores and differences in the cannula-induced damage, the "above HPC" represents the best strategy to reach the ventral hippocampus with high precision and minimal damage.

3.3. Behavioral tests

The mechanical damage of the brain tissue along the route of the cannula insertion, although reduced with our novel implantation strategies, is still present. In order to verify that it did not cause any major impairment, a new and independent batch of epileptic rats (n = 10) was bilaterally implanted with cannulas using the "above HPC" strategy, received injection of IBO and was tested for memory, locomotion and anxiety level. Not implanted naïve rats served as controls (n = 8).

The novel object location test investigates reference memory and spatial learning, which relies heavily on hippocampal activity [30]. It measures the spontaneous tendency of rodents to spend less time exploring a familiar object and their capabilities to recognize when an object has been relocated. Performing the memory test phase at different time intervals from the training session may provide valuable insight regarding the type of memory deficit (short-, intermediate- and long-

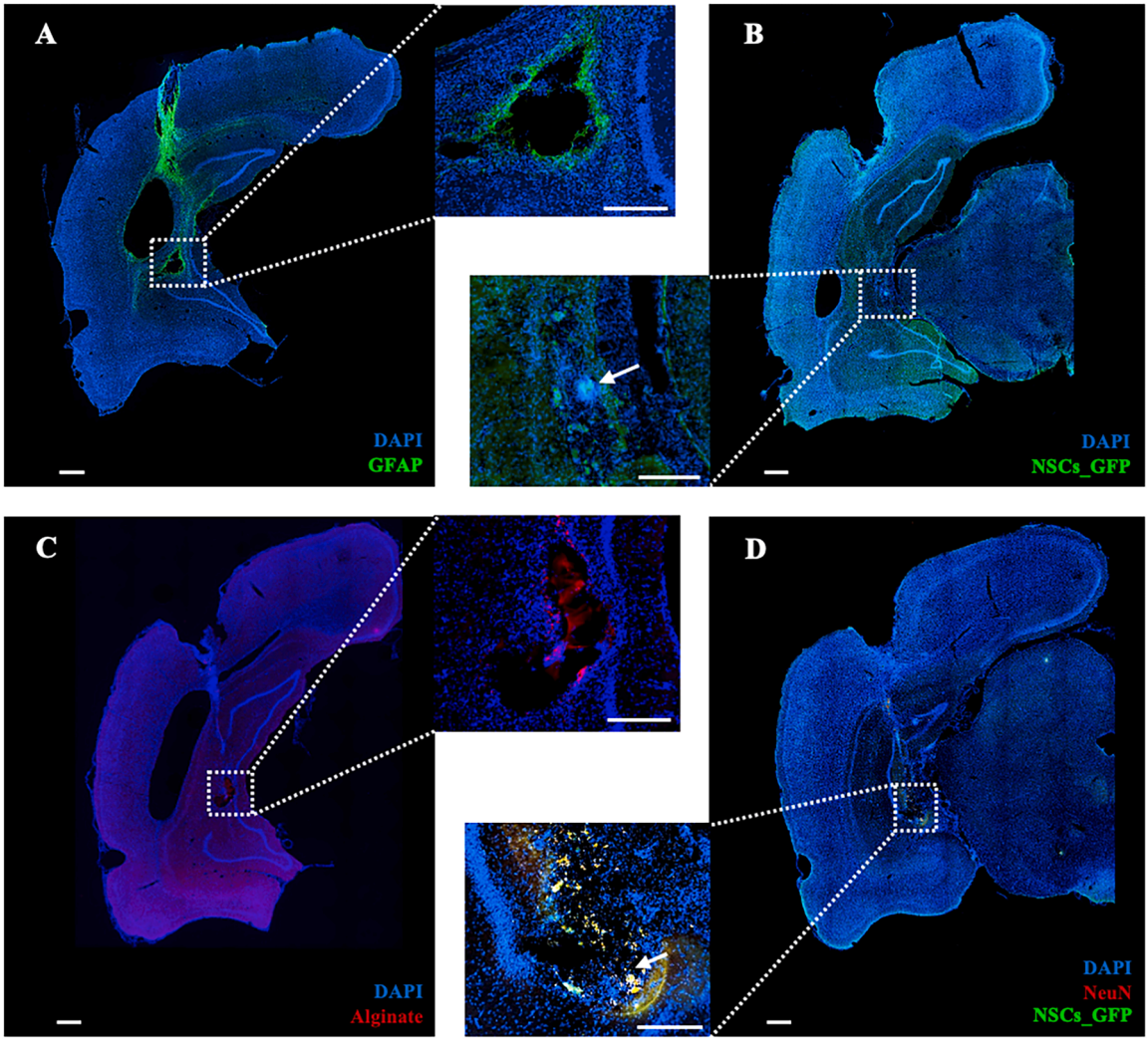

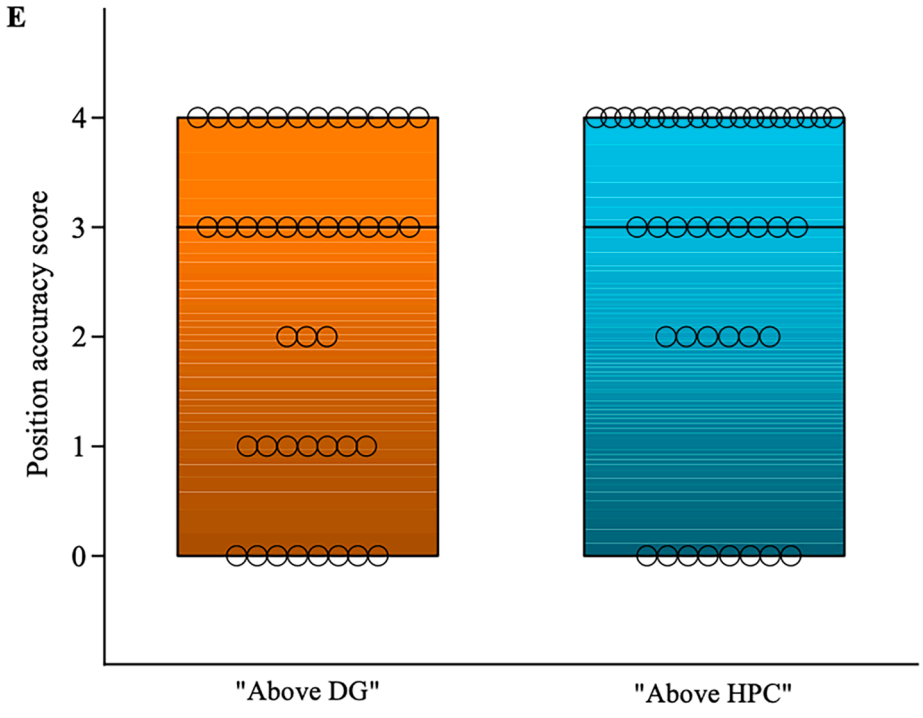

(caption on next page)

Fig. 3. Multiple injections in vCA3 of epileptic rats. Representative immunofluorescence coronal brain sections of epileptic rats 8 (**A**) or 13 (**B**, **C**, **D**) weeks post last injection. (**A**) Epileptic rat injected with IBO using "above DG" strategy; GFAP marks astrocytes (green) and DAPI marks nuclei (blue). In the inset, a magnification shows the lesion induced by the cytotoxic agent IBO. (**B**) Epileptic rat injected with IBO followed by NSCs infusion using the "above HPC" strategy; GFP marks the NSCs (green) and DAPI marks nuclei (blue). In the inset, an arrow points to the injection site. (**C**) Epileptic rat injected with IBO followed by alginate using the "above HPC" strategy; alginate is marked with Alexa Fluor 568 (red) and DAPI marks nuclei (blue). In the inset, it is possible to appreciate that alginate makes a hydrogel filling the IBO-induced lesion. (**D**) Epileptic rat injected with IBO followed by NSCs plus alginate using the "above HPC" strategy; GFP marks the NSCs (green), NeuN marks mature neurons (red) and DAPI marks nuclei (blue), while alginate was unmarked. In the inset, an arrow points a differentiated injected NSC. Main images acquired with 10x objective, scale bars 500 μm; insets acquired at 20x magnification, scale bars 250 μm. (**E**) Box plot representing the position accuracy score, showing the success of both strategies. The open circles represent the performance of each cannula implant. DAPI: 4,6-Diamidino-2-phenylindole; DG: dentate gyrus; GFAP: glial fibrillary acidic protein; GFP: green fluorescent protein; HPC: hippocampus; IBO: ibotenic acid; NSCs: neural stem cells.

term; Supplementary **Fig. S1A**) [31,32]. Our results revealed no statistical difference between implanted epileptic compared to not implanted naïve rats in the time spent on the relocated object at all time points (2 h — naïve w/o cannulas: 21.88 ± 3.69 s; TLE + IBO w/ cannulas: 16.55 ± 1.21 s; 6 h — naïve w/o cannulas: 19.35 ± 3.47 s; TLE + IBO w/ cannulas: 17.33 ± 2.41 s; 24 h — naïve w/o cannulas: 21.24 ± 5.41 s; TLE + IBO w/ cannulas: 14.75 ± 2.59 s; $p > 0.05$ at all time points, Mann-Whitney *U* test; Fig. 5**A**), suggesting no impairments in the short-, intermediate-, and long-term memory caused by cannula-induced damage.

The open field test is commonly used to investigate locomotor and exploratory behavior [33], but it is also validated for the measurement of anxiety level [34]. Interestingly, no significant difference was found between the two experimental groups in the percentage of time spent in the different zones of the arena, suggesting no impairments in the anxiety level (Periphery — naïve w/o cannulas: 68.97 ± 3.18 %; TLE + IBO w/ cannulas: 57.55 ± 4.80 %; Middle — naïve w/o cannulas: 28.06 ± 2.88 %; TLE + IBO w/ cannulas: 37.68 ± 4.41 %; Center — naïve w/o cannulas: 2.97 ± 0.47 %; TLE + IBO w/ cannulas: 4.77 ± 0.66 %; Corners — naïve w/o cannulas: 4.07 ± 0.96 %; TLE + IBO w/ cannulas: 5.66 ± 1.80 %; $p > 0.05$ Mann-Whitney *U* test; Fig. 5**B**).

We evaluated the total distance travelled as indicator of motor activity in the open field test. Implanted epileptic rats did not perform worse than not implanted naïve rats, suggesting that cannula-induced damage did not alter the locomotor performance. Actually, as expected [35,36], epileptic rats manifested a higher motor activity and displayed a hyperactive behavior compared to naïve rats (Day1 — naïve w/o cannulas: 29.83 ± 2.25 m; TLE + IBO w/ cannulas: 59.43 ± 3.92 m. Day2 — naïve w/o cannulas: 25.87 ± 3.36 m; TLE + IBO w/ cannulas: 60.66 ± 4.92 m; $p < 0.0001$, two-way ANOVA followed by Dunn-Sidak *post-hoc* test; Fig. 5**C**).

Light/dark box is commonly used to test innate anxiety-like behavior [37]. The rat was placed in the center of the light compartment box (Supplementary **Fig. S1C**), and the latency of the first entry into the dark room, the number of entries, and the time spent in the dark zone were measured. The results demonstrated no statistically significant differences between groups (Latency — naïve w/o cannulas: 17.25 ± 9.89 s; TLE + IBO w/ cannulas: 20.33 ± 4.73 s. Number of entries — naïve w/o cannulas: 7.75 ± 0.84; TLE + IBO w/ cannulas: 7.33 ± 1.79. Time in the dark zone — naïve w/o cannulas: 331.87 ± 14.25 s; TLE + IBO w/ cannulas: 300.11 ± 41.79 s; $p > 0.05$ Mann-Whitney *U* test; Fig. 5**D**) suggesting that the cannula-induced damage does not increase anxiety level in implanted compared to not implanted rats.

4. Discussion and conclusions

In the present study we proposed two novel approaches, the "above DG" and the "above HPC" strategies, to implant guide cannulas at a greater distance from the target area than the traditional approaches [9,10] in order to perform injections with minimal damage. In our preclinical study [3] aiming at investigating a novel therapy to treat TLE, we needed to perform multiple injections into the ventral hippocampus, a deep brain area important for learning and memory, and whose lesion may cause cognitive and affective impairments. Our results demonstrated that multiple injections in vCA3 were performed with high and comparable precision using the two novel strategies, leaving the ventral hippocampus undamaged and therefore avoiding impairment in memory and locomotor performances or in anxiety levels.

Before conducting these experiments, we evaluated the cannula "yes" or "no" options. We considered, indeed, that implanting the guide cannula might result in a greater damage due to its larger diameter compared to the thin infusion needle. However, performing infusions without the guide cannula would increase the risk of compromising the whole study. As we aimed at reaching areas located deep in the brain, the error due to the needle deviation during the insertion would become important, progressively reducing the precision of injections. This is a critical aspect in particular in our study in which it was important that the agents injected at different times would reach exactly the same spot to be functional for the therapy under investigation. For example, it was important that alginate would perfectly fill the lesion previously caused by IBO, or that NSCs would reach the precise area were IBO previously killed epileptic endogenous cells. The use of the needle inserted through the cannula would inevitably result in the same level of damage while repeatedly reaching the same target with consistency and reproducibility. Using a guide cannula offers further advantages, including a shorter surgical procedure for infusions, meaning shorter anaesthesia and recovery time, improving animal welfare. In addition, this approach enables the injection of a higher number of animals in a single day during experimental procedures, a positive aspect when conducting preclinical studies. Finally, being more precise, it required fewer animals to reach the good experimental sample size representing a further 3Rs strategy [38].

The two new strategies proposed in our study foresee a bigger distance between the guide cannula and the target area (approximately 4 mm from the vCA3 for the "above HPC" strategy and 2 mm for the "above DG" strategy) with respect to the more standard procedures (0–1 mm). A few studies have reported a distance between the guide cannula and the target area of 2 mm, similar to the "above DG" strategy we present here; however, the main focus of these studies was elsewhere and a methodological analysis of the precision score or of the cannula-induced damage was not reported [39,40]. Our approaches have the advantage of minimizing the tissue damage and ensuring a reliable distribution of infused substances, such as cells, polymeric scaffold, or lesioning agent in rat brains. This is based on the well-supported findings by Yin and colleagues who demonstrated that maintaining a distance of at least 1 mm between the cannula end and the infusion needle is highly effective for infusions [10]. We did not test the "standard" approach to perform our experiments because one of our tasks was to preserve the hippocampus as much as possible and, for ethical reasons, we were conscious that the "standard" strategy would have caused massive brain damage due to its great invasiveness and to the deep location of the target area [9]. For all these reasons, we avoided the more standard strategy reducing the number of overall animals used.

The degrees of infusion accuracy were based on a working hypothesis. The exact target location was determined first based on the localization of the vCA3 at each specific AP value from the Bregma and then along different AP values to evaluate the area interested in the spreading of the injected substance. The success rate of our implants in reaching the target area was 80.49 %, with varying degrees of accuracy observed across multiple injections. The target area, vCA3, is located deep within

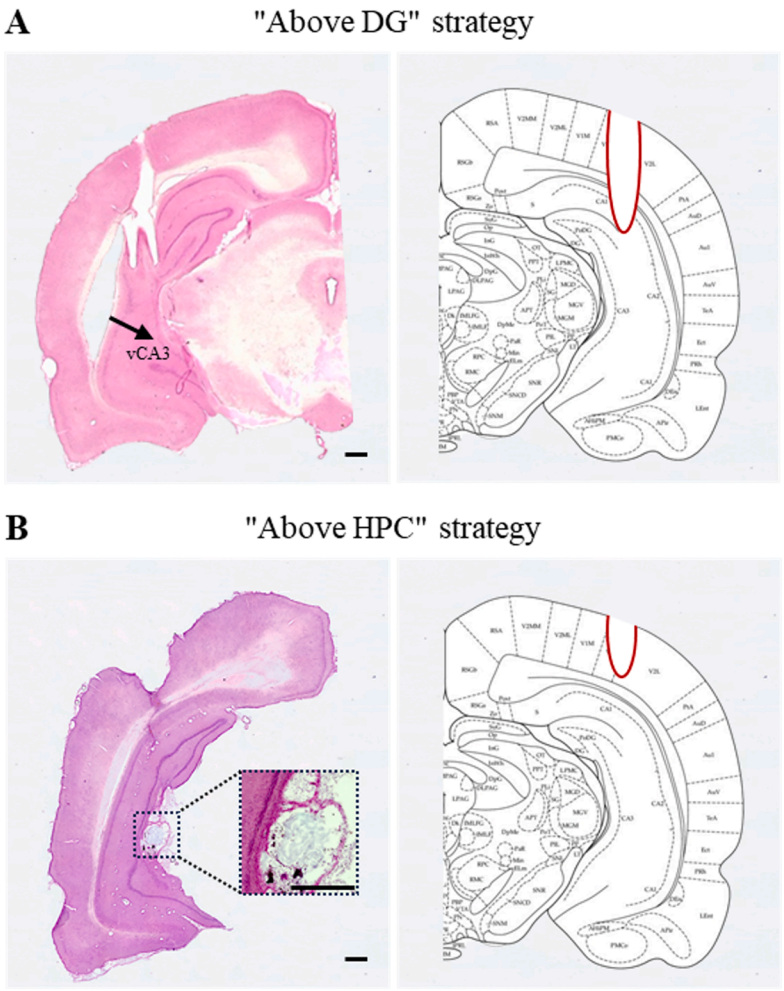

(caption on next page)

Fig. 4. Cannula-induced damage. (**A**, **B**) Representative Hematoxylin & Eosin staining of rat brain coronal sections (10x objective) and corresponding coronal brain schemes illustrating the damage (red line) caused by the guide cannula implantation with the "above DG" (**A**) and the "above HPC" (**B**) strategies (modified from Rat Brain Atlas online free version [24] with PowerPoint). In (**A**) the black arrow indicates the trace left by the infusion needle that perfectly reached vCA3. In (**B**) the dotted square marks the vCA3 area where alginate was injected; the inset (20x objective) shows alginate filling the hole created by IBO. Scale bars: 500 μm. (**C**) The bar chart shows the percentage of damaged (grey) or intact (pink) hippocampi. When undamaged (100 % in the "above HPC" strategy) the damage is limited to the cortex. DG: dentate gyrus; HPC: hippocampus; vCA3: ventral Cornu Ammonis 3.

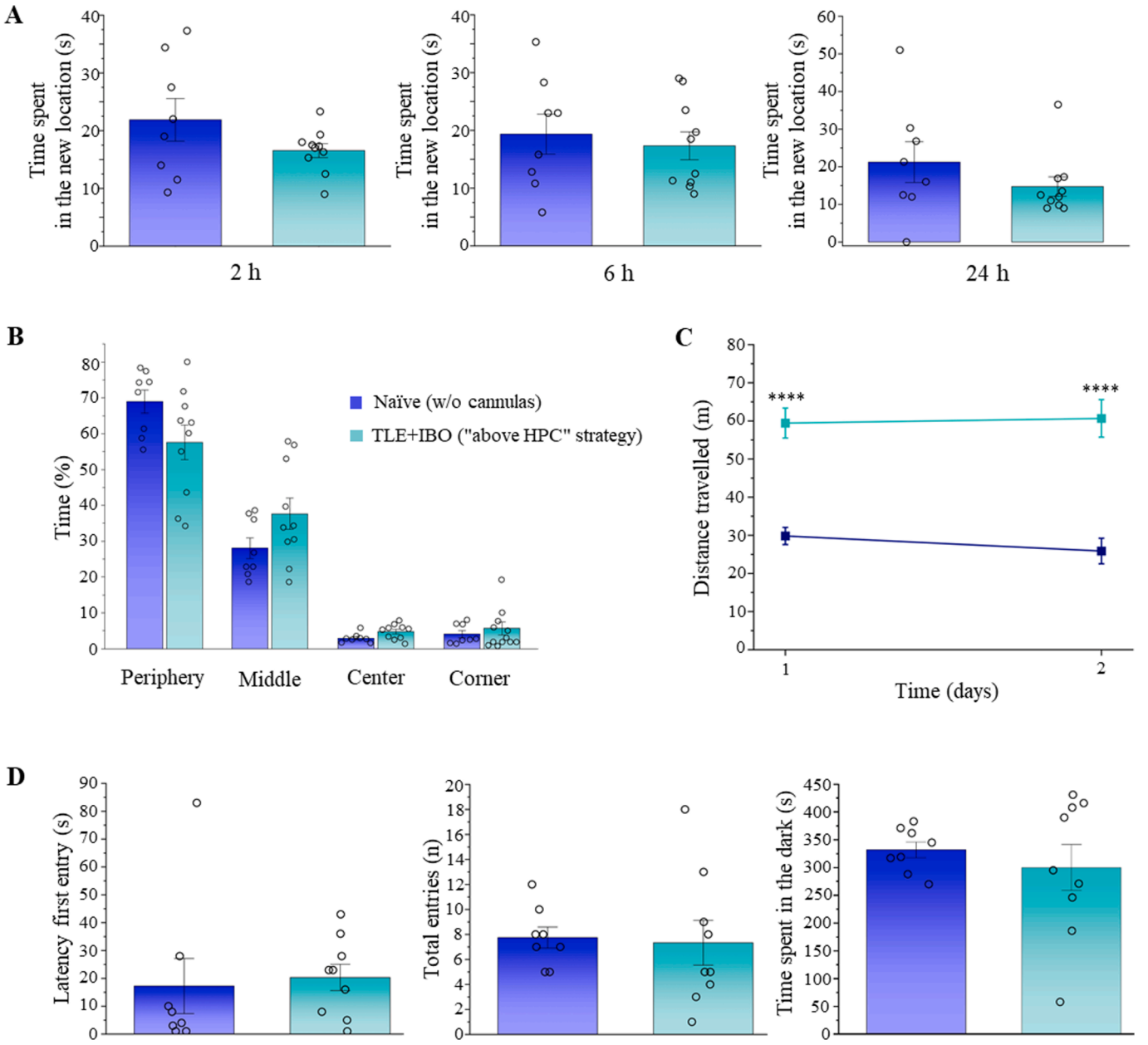

Fig. 5. Behavioral tests. (**A**) Bar graphs of the time spent in the object replaced in the new location show no differences in memory test between epileptic rats implanted with guide cannulas using the "above HPC" strategy and not implanted naïve rats. (**B**) Bar graphs show the percentage of time spent in the different arena zones (periphery, middle, center and corners) on day 1 of the open field test as indicator of the anxiety level. (**C**) Distance travelled by implanted/injected epileptic rats and not implanted naïve rats on day 1 and 2 of the open field test indicates locomotion is not compromised by cannula implantation. ****$p < 0.0001$, two-way ANOVA Dunn-Sidak *post-hoc* test. (**D**) Bar graphs showing the latency of the first entry (left), the number of entries (middle) and the time spent in the dark area (right) as indicators of anxiety reveal no differences between implanted epileptic and not implanted naïve rats. The open circles represent the single animal values. HPC: hippocampus; IBO: ibotenic acid; TLE: temporal lobe epilepsy.

the brain, close to the inter-thalamic space, a brain area that is affected by structural deformation caused by ventricular dilation and hippocampal atrophy in TLE rats [41]. The vCA3 was not reached in only 19.51 % of cases, in which infusions fell, indeed, into the inter-thalamic space. This observation suggests that the precision score that we obtained in TLE rats would likely come out even better in naïve rats, as the deformation caused by the pathology would not be present.

As expected, the mechanical damage induced by the cannulas implanted using the two novel strategies was limited or nearby the cortex, mainly leaving the hippocampus intact. Our behavioral tests

showed the good performance of implanted rats in locomotor, memory, and anxiety tests, suggesting that the cannula-induced damage implanted using the "above HPC" strategy did not compromise cognitive tasks. These results are even more relevant considering that to reduce the number of total animals, we performed behavioral tests limitedly in the worst-case scenario (lesioned epileptic implanted rats) and in the best-case scenario (naïve not implanted rats). The lack of behavioral impairments in lesioned rats is due most likely to the low amount of toxic agent injected.

Our data show that epileptic rats increased locomotor activity (travelled distance in the open field test increased) indicating a hyperactive behavior as expected [36], a data that Pearson et al. observed for the kainite model but not for the pilocarpine model [42]. The study by Pearson et al. reports cognitive impairments in the kainate model of TLE both in the novel object location and in the novel object recognition tests, while in the pilocarpine model, cognitive impairment was not observed in the novel object location [42] in line with our results. We evaluated anxiety level measuring the percentage of time rats spent in different areas of the arena in the open field test, finding no difference between not implanted naïve rats and implanted epileptic rats; these data are in line with what observed by Pearson et al. [42], but not with data shown by Muller et al. who also reported different results in the light/dark box test [36]. The reason why we obtained no difference in the anxiety level between naïve and epileptic rats is probably because we did an extensive rat handling: rats were visited and handled weekly from their arrival to the week before behavioral tests, and daily during the two weeks while behavioral tests were performed. Handling procedure and frequency were identical for experimental and control groups. Overall, our data showing no differences between implanted and not implanted rats support our conclusion that cannula-induced damage does not compromise locomotion, cognition and anxiety, in line with other studies [43,44]. It is worth to point out that the damage left by the cannula implanted with the "above HPC" strategy involves mainly the cortex, in particular, at this Bregma level, the visual cortex. The time spent on the novel object is not different between implanted and not implanted rats suggesting that there is a voluntary interaction of the rat with the object based on which we can speculate rats can see the object indicating no major visual impairment due to the cannula-induced damage. However, we cannot exclude that specific test for finer visual impairments would unveil a deficit in these animals.

Our results support the efficacy of our strategies for the implantation of guide cannulas in achieving the target zone located deep in the rat brain with high precision and minimal damage. In particular, between the two proposed strategies, the "above HPC" should be preferred as it leaves the whole hippocampus undamaged increasing the translational relevance for preclinical studies on TLE or other neurological disorders.

Funding

This work was supported by the European Union's Horizon 2020 FET Proactive project "Hybrid Enhanced Regenerative Medicine Systems" (HERMES, GA n.824164) acknowledged to GC, ID and GP. #NEXTGENERATIONEU (NGEU) and funded by the Ministry of University and Research (MUR), National Recovery and Resilience Plan (NRRP), project MNESYS (PE0000006) – A Multiscale integrated approach to the study of the nervous system in health and disease (DN. 1553 11.10.2022) is acknowledged to ID and FC.

Declaration of competing interest

The authors declare that they have no known competing financial interests or personal relationships that could have appeared to influence the work reported in this paper.

Acknowledgements

The Authors thank Mr. Claudio Frigeri for the technical support in the homemade guide cannulas production.

Author Contribution: First draft writing SB and GC, manuscript editing, experiments and analysis all Authors.

All Authors have read and agreed to the published version of the manuscript.

Appendix A. Supplementary data

Supplementary data to this article can be found online at https://doi.org/10.1016/j.ymeth.2025.03.005.

Data availability

Data will be available upon request.

References

[1] J.C. DaCosta, M.W. Portuguez, D.R. Marinowic, L.P. Schilling, C.M. Torres, D. I. DaCosta, M.J.M. Carrion, E.F. Raupp, D.C. Machado, R.B. Soder, S.L. Lardi, B. Garicochea, Safety and seizure control in patients with mesial temporal lobe epilepsy treated with regional superselective intra-arterial injection of autologous bone marrow mononuclear cells, J. Tissue Eng. Regen. Med. 12 (2018), https://doi.org/10.1002/term.2334.

[2] A. Ramos-Fresnedo, C. Perez-Vega, R.A. Domingo, S.J. Lee, R.B. Perkerson, A. C. Zubair, K. Takahisa, W. Tatum, A. Quinones-Hinojosa, E.H. Middlebrooks, S. S. Grewal, Mesenchymal stem cell therapy for focal epilepsy: A systematic review of preclinical models and clinical studies, Epilepsia 63 (7) (2022) 1607–1618, https://doi.org/10.1111/epi.17266.

[3] EU-H2020 FET Proactive HERMES project. Eurokleis, HERMES project website. https://www.eurokleis.com/project/hermes/ (last accessed 3 March 2025).

[4] A. Holguin, M.G. Frank, J.C. Biedenkapp, K. Nelson, D. Lippert, L.R. Watkins, J. W. Rudy, S.F. Maier, Characterization of the temporo-spatial effects of chronic bilateral intrahippocampal cannulae on interleukin-1β, J. Neurosci. Methods. 161 (2007) 265–272, https://doi.org/10.1016/j.jneumeth.2006.11.014.

[5] L.A. Crane, S.D. Glick, Simple cannula for repeated intracerebral drug administration in rats, Pharmacol, Biochem. Behav. 10 (1979) 799–800, https://doi.org/10.1016/0091-3057(79)90336-8.

[6] S.L. Peterson, Drug microinjection in discrete brain regions, Kopf Carrier. 50 (1998) 1–6. https://kopfinstruments.com/app/uploads/2015/04/Carrier50.pdf.

[7] A.R. Abela, Y. Chudasama, Noradrenergic α_{2A}-receptor stimulation in the ventral hippocampus reduces impulsive decision-making, Psychopharmacology (Berl) 231 (2014) 521–531, https://doi.org/10.1007/s00213-013-3262-y.

[8] A.H. Emam, N. Hajesfandiari, S. Shahidi, A. Komaki, M. Ganji, A. Sarihi, Modulation of nociception by medial pre-optic area orexin a receptors and its relation with morphine in male rats, Brain Res. Bull. 127 (2016) 141–147, https://doi.org/10.1016/j.brainresbull.2016.09.009.

[9] D.M. Kokare, G.P. Shelkar, C.D. Borkar, K.T. Nakhate, N.K. Subhedar, A simple and inexpensive method to fabricate a cannula system for intracranial injections in rats and mice, J. Pharmacol. Toxicol. Methods. 64 (2011) 246–250, https://doi.org/10.1016/j.vascn.2011.08.002.

[10] D. Yin, J. Forsayeth, K.S. Bankiewicz, Optimized cannula design and placement for convection-enhanced delivery in rat striatum, J. Neurosci. Methods. 187 (2010) 46–51, https://doi.org/10.1016/j.jneumeth.2009.12.008.

[11] L. Hayn, L. Deppermann, M. Koch, Reduction of the foreign body response and neuroprotection by apyrase and minocycline in chronic cannula implantation in the rat brain, Clin. Exp. Pharmacol. Physiol. 44 (2017) 313–323, https://doi.org/10.1111/1440-1681.12703.

[12] C. Kilkenny, W.J. Browne, I.C. Cuthill, M. Emerson, D.G. Altman, Improving Bioscience Research Reporting: The ARRIVE Guidelines for Reporting Animal Research, PLoS Biol. 8 (2010) e1000412, https://doi.org/10.1371/journal.pbio.1000412.

[13] N. Percie Du Sert, V. Hurst, A. Ahluwalia, S. Alam, M.T. Avey, M. Baker, W. J. Browne, A. Clark, I.C. Cuthill, U. Dirnagl, M. Emerson, P. Garner, S.T. Holgate, D.W. Howells, N.A. Karp, S.E. Lazic, K. Lidster, C.J. MacCallum, M. Macleod, E. J. Pearl, O.H. Petersen, F. Rawle, P. Reynolds, K. Rooney, E.S. Sena, S. D. Silberberg, T. Steckler, H. Würbel, The ARRIVE guidelines 2.0: Updated guidelines for reporting animal research, PLoS Biol. 18 (2020) e3000410, https://doi.org/10.1371/journal.pbio.3000410.

[14] ARRIVE guidelines. https://arriveguidelines.org (last accessed 10 October 2024).

[15] European Union, Animals in science, EU actions for the protection of animals used for scientific purposes. https://environment.ec.europa.eu/topics/chemicals/animals-science_en (last accessed 3 March 2025).

[16] V. Baumans, P.F. Brain, H, Brugére, P. Clausing, T. Jeneskog, G. Perretta, Pain and distress in laboratory rodents and lagomorphs: Report of the Federation of European Laboratory Animal Science Associations (FELASA) Working Group on Pain and Distress accepted by the FELASA Board of Management November 1992, Lab. Anim. 28 (1994) 97–112. https://doi.org/10.1258/002367794780745308.

[17] K. Lidster, J.G. Jefferys, I. Blümcke, V. Crunelli, P. Flecknell, B.G. Frenguelli, W. P. Gray, R. Kaminski, A. Pitkänen, I. Ragan, M. Shah, M. Simonato, A. Trevelyan, H. Volk, M. Walker, N. Yates, M.J. Prescott, Opportunities for improving animal welfare in rodent models of epilepsy and seizures, J. Neurosci. Methods. 260 (2016) 2–25, https://doi.org/10.1016/j.jneumeth.2015.09.007.

[18] S.G. Sotocina, R.E. Sorge, A. Zaloum, A.H. Tuttle, L.J. Martin, J.S. Wieskopf, J. C. Mapplebeck, P. Wei, S. Zhan, S. Zhang, J.J. McDougall, O.D. King, J.S. Mogil, The Rat Grimace Scale: A Partially Automated Method for Quantifying Pain in the Laboratory Rat via Facial Expressions, Mol. Pain. 7 (2011) 1744–8069-7–55, https://doi.org/10.1186/1744-8069-7-55.

[19] V. Oliver, D. De Rantere, R. Ritchie, J. Chisholm, K.G. Hecker, D.S.J. Pang, Psychometric Assessment of the Rat Grimace Scale and Development of an Analgesic Intervention Score, PLoS One 9 (2014) e97882, https://doi.org/10.1371/journal.pone.0097882.

[20] S. Ghosal, A. Nunley, P. Mahbod, A.G. Lewis, E.P. Smith, J. Tong, D.A. D'Alessio, J. P. Herman, Mouse handling limits the impact of stress on metabolic endpoints, Physiol. Behav. 150 (2015) 31–37, https://doi.org/10.1016/j.physbeh.2015.06.021.

[21] R.J. Racine, Modification of seizure activity by electrical stimulation: II, Motor Seizure, Electroencephalography and Clinical Neurophysiology. 32 (1972) 281–294, https://doi.org/10.1016/0013-4694(72)90177-0.

[22] R.B. Kazanskaya, A.V. Lopachev, T.N. Fedorova, R.R. Gainetdinov, A.B. Volnova, A low-cost and customizable alternative for commercial implantable cannula for intracerebral administration in mice, Hardw.x. 8 (2020) e00120, https://doi.org/10.1016/j.ohx.2020.e00120.

[23] G. Paxinos, C. Watson, Paxino's and Watson's The rat brain in stereotaxic coordinates, seventh ed., Elsevier/AP, Amsterdam, Boston, 2014.

[24] Matt Gaidica, Rat Brain Atlas. https://labs.gaidi.ca/rat-brain-atlas/?ml=-4.5&ap=-5.5&dv=-6.2 (last accessed 3 March 2025).

[25] G. Palazzolo, N. Broguiere, O. Cenciarelli, H. Dermutz, M. Zenobi-Wong, Ultrasoft Alginate Hydrogels Support Long-Term Three-Dimensional Functional Neuronal Networks, Tissue Eng. A 21 (2015) 2177–2185, https://doi.org/10.1089/ten.tea.2014.0518.

[26] G. Della Rosa, N. Gostynska, J.W. Ephraim, S. Marras, M. Moroni, N. Tirelli, G. Panuccio, G. Palazzolo, Magnesium vs. sodium alginate as precursors of calcium alginate: Mechanical differences and advantages in the development of functional neuronal networks, Carbohydr. Polym. 342 (2024) 122375, https://doi.org/10.1016/j.carbpol.2024.122375.

[27] S. Dolci, A. Pino, V. Berton, P. Gonzalez, A. Braga, M. Fumagalli, E. Bonfanti, E., Malpeli, G., Pari, F., Zorzin, S., Amoroso, C., Moscon, D., Rodriguez, F.J., Fumagalli, G., Bifari, F., Decimo, I., 2017. High Yield of Adult Oligodendrocyte Lineage Cells Obtained from Meningeal Biopsy, Front. Pharmacol. 8 (2017) 703. https://doi.org/10.3389/fphar.2017.00703.

[28] A. Yoshimura, M. Ito, Resolution of inflammation and repair after ischemic brain injury, Neurosciences 7 (2020) 264–276, https://doi.org/10.20517/2347-8659.2020.22.

[29] KellyBullockArt, Rat Brain. https://p3d.in/48zSR/wireonxray (last accessed 10 October 2024).

[30] J.K. Denninger, B.M. Smith, E.D. Kirby, Novel Object Recognition and Object Location Behavioral Testing in Mice on a Budget, JoVE. 141 (2018), https://doi.org/10.3791/58593.

[31] G. Lippi, C.C. Fernandes, L.A. Ewell, D. John, B. Romoli, G. Curia, S.R. Taylor, E. P. Frady, A.B. Jensen, J.C. Liu, M.M. Chaabane, C. Belal, J.L. Nathanson, M. Zoli, J. K. Leutgeb, G. Biagini, G.W. Yeo, D.K. Berg, MicroRNA-101 Regulates Multiple Developmental Programs to Constrain Excitation in Adult Neural Networks, Neuron 92 (2016) 1337–1351, https://doi.org/10.1016/j.neuron.2016.11.017.

[32] S. Stough, J.L. Shobe, T.J. Carew, Intermediate-term processes in memory formation, Curr. Opin. Neurobiol. 16 (2006) 672–678, https://doi.org/10.1016/j.conb.2006.10.009.

[33] R.N. Walsh, R.A. Cummins, The open-field test: A critical review, Psychol. Bull. 83 (1976) 482–504, https://doi.org/10.1037/0033-2909.83.3.482.

[34] A.K. Kraeuter, P.C. Guest, Z. Sarnyai, The Open Field Test for Measuring Locomotor Activity and Anxiety-Like Behavior, Methods Mol. Biol. 2019 (1916) 99–103, https://doi.org/10.1007/978-1-4939-8994-2_9.

[35] C. Brandt, A. Gastens, M. Sun, M. Hausknecht, W. Loscher, Treatment with valproate after status epilepticus: Effect on neuronal damage, epileptogenesis, and behavioral alterations in rats, Neuropharmacology 51 (2006) 789–804, https://doi.org/10.1016/j.neuropharm.2006.05.021.

[36] C.J. Müller, I. Gröticke, M. Bankstahl, W. Löscher, Behavioral and cognitive alterations, spontaneous seizures, and neuropathology developing after a pilocarpine-induced status epilepticus in C57BL/6 mice, Exp. Neurol. 219 (2009) 284–297, https://doi.org/10.1016/j.expneurol.2009.05.035.

[37] A.E. Arrant, N.L. Schramm-Sapyta, C.M. Kuhn, Use of the light/dark test for anxiety in adult and adolescent male rats, Behav. Brain Res. 256 (2013) 119–127, https://doi.org/10.1016/j.bbr.2013.05.035.

[38] B. Ferry, D. Gervasoni, Improving Stereotaxic Neurosurgery Techniques and Procedures Greatly Reduces the Number of Rats Used per Experimental Group—A Practice Report, Anim. 11 (2021) 2662, https://doi.org/10.3390/ani11092662.

[39] E.M. Purvis, A.K. Klein, A. Ettenberg, Lateral habenular norepinephrine contributes to states of arousal and anxiety in male rats, Behav. Brain Res. 347 (2018) 108–115, https://doi.org/10.1016/j.bbr.2018.03.012.

[40] K. Shelton, K. Bogyo, T. Schick, A. Ettenberg, Pharmacological modulation of lateral habenular dopamine D2 receptors alters the anxiogenic response to cocaine in a runway model of drug self-administration, Behav. Brain Res. 310 (2016) 42–50, https://doi.org/10.1016/j.bbr.2016.05.002.

[41] H.G. Niessen, F. Angenstein, S. Vielhaber, C. Frisch, A. Kudin, C.E. Elger, H. Heinze, H. Scheich, W.S. Kunz, Volumetric Magnetic Resonance Imaging of Functionally Relevant Structural Alterations in Chronic Epilepsy after Pilocarpine-induced Status Epilepticus in Rats, Epilepsia 46 (2005) 1021–1026, https://doi.org/10.1111/j.1528-1167.2005.60704.x.

[42] J.N. Pearson, K.M. Schulz, M. Patel, Specific alterations in the performance of learning and memory tasks in models of chemoconvulsant-induced status epilepticus, Epilepsy Res. 108 (2014) 1032–1040, https://doi.org/10.1016/j.eplepsyres.2014.04.003.

[43] B. Seyer, V. Pham, A.L. Albiston, S.Y. Chai, Cannula implantation into the lateral ventricle does not adversely affect recognition or spatial working memory, Neurosci Lett. 628 (2016) 171–178, https://doi.org/10.1016/j.neulet.2016.06.034.

[44] F. Hernández-López, J.F. Rodríguez-Landa, A. Puga-Olguín, L.J. Germán-Ponciano, E. Rivadeneyra-Domínguez, B. Bernal-Morales, Analysis of activity and motor coordination in rats undergoing stereotactic surgery and implantation of a cannula into the dorsal hippocampus, Neurologia. 32 (2017) 579–586, https://doi.org/10.1016/j.nrl.2016.03.004.